

New solution for damaged porous RC cantilever beams strengthening by composite plate

Rabahi Abderezak^{1,2}, Tahar Hassaine Daouadji^{*1,2} and Benferhat Rabia^{1,2}

¹ Civil Engineering Department, University of Tiaret, Algeria

² Laboratory of Geomatics and Sustainable Development, University of Tiaret, Algeria

(Received April 6, 2020, Revised November 23, 2020, Accepted April 30, 2021)

Abstract. This research presents a careful theoretical investigation on interfacial stresses in damaged porous RC cantilever beams strengthened with externally bonded composite plate (several types of composites have been used). The model is based on equilibrium and deformations compatibility requirements in and all parts of the strengthened cantilever beam, i.e., the damaged porous concrete cantilever beam, the perfect and/or imperfect composite plate and the adhesive layer. The analytical predictions are compared with other existing solutions and which shows a very good agreement of the results. It is shown that both the normal and shear stresses at the interface are influenced by the material and geometry parameters of the composite beam. In the end, I think this research is very useful for understanding the mechanical behavior of the interface and the design of the hybrid structures.

Keywords: composite plate; damaged RC cantilever beam; interfacial stresses; porosity; strengthening

1. Introduction

The composite materials have been recognized as new innovative materials for concrete rehabilitation and retrofit. Since concrete is poor in tension, a beam without any form of reinforcement will fail when subjected to a relatively small tensile load. Therefore, the bonding of FRP plate to reinforced concrete (RC) structure is an effective solution to increase its overall strength (Smith and Teng 2002, Tounsi *et al.* 2008, Chergui *et al.* 2019, Chedad *et al.* 2018, Daouadji 2013 and Yang and Wu 2007). In such plated beams, tensile forces develop in the bonded plate and these have to be transferred to the original beam via interfacial shear and normal stresses. Consequently, the debonding of FRP plates bonded to reinforced concrete beams is believed to be initiated by the stress concentration in the adhesive layer (Tounsi 2006, Hamrat *et al.* 2020, Tahar *et al.* 2020, Nejadi and Mohammadimehr 2020, Panjehpour *et al.* 2016, AkhavanAlavi *et al.* 2019, Mohammadimehr *et al.* 2016a and Rabahi *et al.* 2016). Accurate predictions of the interfacial stresses are prerequisite for designing against debonding failures.

The aim of this paper is to study the mechanical behavior of damaged porous reinforced concrete beams reinforced by composite materials. This repair method consists of strengthening composite plates on these beams. In recent years, several works have been carried out on the rehabilitation method (Atmane *et al.* 2015, Sharif *et al.* 2020, Antar *et al.* 2019, Guenaneche and Tounsi 2014,

*Corresponding author, Professor, E-mail: daouadjitahar@gmail.com; tahar.daouadji@univ-tiaret.dz

Mohammadimehr *et al.* 2020, Adim *et al.* 2016a, b, Benferhat *et al.* 2016a, Tahar *et al.* 2019, Abderezak *et al.* 2018b, 2021a, Panjehpour *et al.* 2014, Mohammadimehr *et al.* 2016b, 2017b, 2018b, Rabia *et al.* 2019, 2021, Abualnour *et al.* 2019, Alimirzaei *et al.* 2019, Tounsi *et al.* 2020, Chikr *et al.* 2019). Thus, composites are therefore a promising solution to the problem of rehabilitation. However, the most important failure mode of these reinforced beams is the separation of the composite plate (peeling off effect) (Benyoucef *et al.* 2007, Boulal *et al.* 2020, Mahi *et al.* 2014, Daouadji 2017, Krour *et al.* 2014, Mohammadimehr *et al.* 2017c, Benferhat *et al.* 2016b, Benhenni *et al.* 2018, Bensattalah *et al.* 2018, Bouakaz *et al.* 2014, Ghorbanpour *et al.* 2016, Zohra *et al.* 2021, Abderezak *et al.* 2021a, b, Mohammadimehr and Alimirzaei 2016a, Mohammadimehr *et al.* 2018a, Daouadji *et al.* 2008, Rabahi *et al.* 2014, Belkacem *et al.* 2016a and Tayeb *et al.* 2020), due to the high interface stresses near the edge of the glued plate. In this paper, an improved method for calculating interface stresses has been developed in a damaged porous RC cantilever beam strengthening by several types of composite material. The anisotropic nature of composite materials was taken into account in the theoretical analysis by assuming a linear distribution of stresses across the thickness of the adhesive layer. We have noticed through the results obtained that the maximum interface constraints calculated by the present method coincide perfectly with those from the literature (Mohammadimehr *et al.* 2018c, Mohammadimehr and Shahedi 2016, Adim *et al.* 2016b, Benferhat *et al.* 2016c, Hussain *et al.* 2020, Mohammadimehr *et al.* 2020, Shahedi and Mohammadimehr 2020, Rostami and Mohammadimehr 2020, Alambeigi *et al.* 2020, Rajabi and Mohammadimehr 2019, Babaeian and Mohammadimehr 2020 Mohammadimehr *et al.* 2017a, Abdelhak *et al.* 2016, Aicha *et al.* 2020, Abderezak *et al.* 2018, Belkacem *et al.* 2018, Tlidji *et al.* 2021, Hadj *et al.* 2021, Benferhat *et al.* 2021, Benhenni *et al.* 2019, Tayeb and Daouadji 2020, Abderezak *et al.* 2020, and Mohammadimehr and Mehrabi 2018b).

Most of the research efforts have focused on strengthening of undamaged RC beams with externally bonded sheets, whereas the interfacial stresses in damaged porous RC cantilever beams strengthened by externally bonded FRP strips has not been fully studied yet. The main objective of the present study is to analyze the interfacial stresses in damaged porous RC cantilever beams strengthened with composite plate; namely for the five types of GFRP, sika wrap, CFRP, sika carbodur and FGM materials. The simple approximate closed-form solutions discussed in this paper provide a useful but simple tool for understanding the interfacial behavior of an externally bonded composite plate on the damaged porous concrete beam with the consideration of the effect of distribution forms of porosity in the case of FGM plate.

2. Theoretical formulation and solutions procedure

2.1 Material properties of the concrete cantilever beams

Damage to the cantilever beams concrete:

The model's Mazars is based on elasticity coupled with isotropic damage and ignores any manifestation of plasticity, as well as the closing of cracks (Mazars and Pijaudier-Cabot 1996). This concept directly describes the loss of rigidity and the softening behavior. The constraint is determined by the following expression

$$\sigma_{ij} = (1 - d)E_{ij}\varepsilon_{ij} \quad 0 < d < 1 \quad (1a)$$

$$\bar{E}_{11} = E_{11}(1 - d) \quad (1b)$$

where \bar{E}_{11} and E_{11} are the elastic constants of damaged and undamaged state, respectively. “ d ” is damaged variable. Hence, the material properties of the damaged beam can be represented by replacing the above elastic constants with the effective ones defined in Eq. (1b).

Porosity of the cantilever beams concrete:

Due to the manufacturing defects of concrete such as the air bubbles “ ϕ ” which are the subject of the subject, the Young’s modulus (E_1) of the imperfect reinforced concrete beam can be written as a function of the volume of the material. The mathematical form of porosity in concrete which can be presented in the form below

$$E_1 = E_b(1 - \phi) \tag{1c}$$

$$\sigma_{ij} = (1 - \phi)E_{ij}\varepsilon_{ij} \tag{1d}$$

Where E_b is the elastic constants of concrete and “ ϕ ” is the index of air bubbles in concrete.

2.2 Mathematical formulation of the present method

Figs. 1 and 2 shows a differential section dx , can be cut out from the composite reinforced concrete damaged cantilever beam. The composite beam is made from three materials: damaged concrete (or damaged reinforced concrete), adhesive layer and composite reinforcement. In the present analysis, all of the materials are assumed to display linear elastic behaviour; the adhesive is assumed to play a role only in transferring the stresses from the concrete to the FRP reinforcement and the stresses in the adhesive layer do not change through the direction of the thickness (Daouadji *et al.* (2016a).

Basic equation of elasticity:

The longitudinal resultant forces, N_1 and N_2 , for the lower adherends is

$$N_1 = b_1 \int_0^{t_1} \sigma_1^N(y) dy \tag{2a}$$

Where σ_1^N is longitudinal normal stresses for the lower adherends, and which can be rewritten in the form

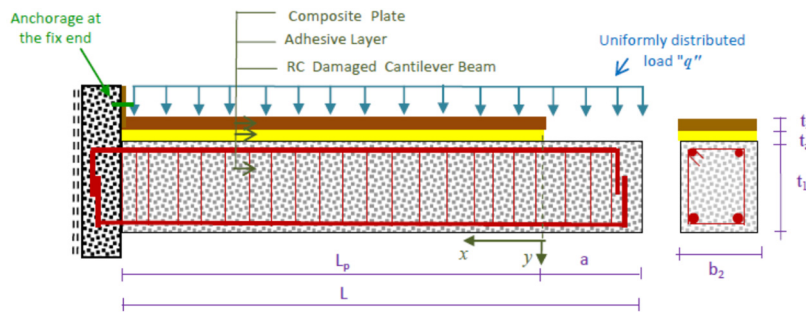


Fig. 1 RC damaged cantilever beam strengthening with composite plate

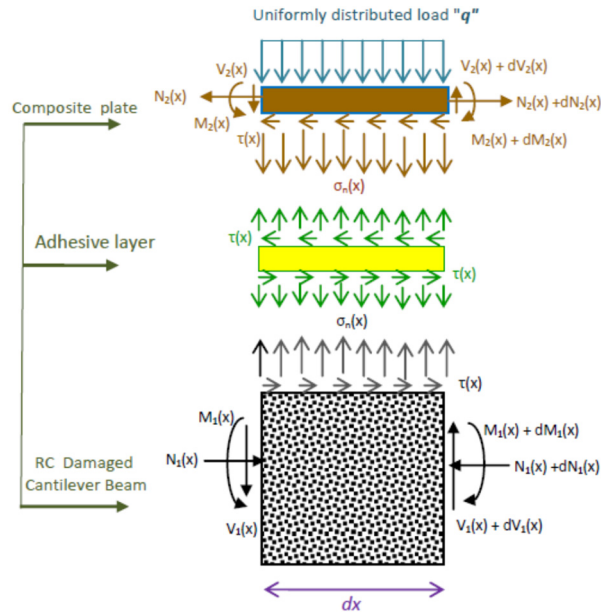


Fig. 2 Forces in an infinitesimal element of an composite strengthened RC damaged cantilever beam

$$N_1 = E_1 b_1 \int_0^{t_1} \frac{dU_1^N}{dx} dy = E_1 A_1 \left(\frac{du_1^N}{dx} - \frac{t_1}{4G_1} \frac{d\tau_a}{dx} \right) \quad (2b)$$

The deformation in concrete in the vicinity of the adhesive layer can be expressed by

$$\varepsilon_1(x) = \frac{du_1(x)}{dx} = \varepsilon_1^M(x) + \varepsilon_1^N(x) \quad (3a)$$

with

$$\varepsilon_1^M(x) = \frac{y_1}{E_1 I_1} M_1(x) \quad (3b)$$

and

$$\varepsilon_1^N(x) = \frac{du_1^N(x)}{dx} = \frac{N_1}{E_1 A_1} + \frac{t_1}{4G_1} \frac{d\tau_a}{dx} \quad (3c)$$

$$\varepsilon_1(x) = \frac{du_1(x)}{dx} = \frac{y_1}{E_1 I_1} M_1(x) + \frac{N_1(x)}{E_1 A_1} + \frac{t_1}{4G_1} \frac{d\tau_a}{dx} \quad (3d)$$

The longitudinal resultant force N_2 for the upper adherends is

$$N_2 = b_2 \int_0^{t_2} \sigma_2^N(y) dy \quad (4a)$$

Where σ_2^N is longitudinal normal stresses for the upper adherends, and which can be rewritten

in the form

$$N_2 = E_2 b_2 \int_0^{t_2} \frac{dU_2^N}{dx} dy' = E_2 A_2 \left(\frac{du_2^N}{dx} + \frac{5t_2}{12G_2} \frac{d\tau_a}{dx} \right) \quad (4b)$$

Based on the theory of laminated sheets, the deformation of the composite sheet in the vicinity of the adhesive layer is given by

$$\varepsilon_2(x) = \frac{du_2(x)}{dx} = \varepsilon_2^M(x) + \varepsilon_2^N(x) \quad (5a)$$

with

$$\varepsilon_2^M(x) = \frac{-y_2}{E_2 I_2} M_2(x) \quad (5b)$$

and

$$\varepsilon_2^N(x) = \frac{du_2^N(x)}{dx} = A'_{11} \frac{N_2(x)}{b_2} - \frac{5t_2}{12G_2} \frac{d\tau_a}{dx} \quad (5c)$$

$$\varepsilon_2(x) = \frac{du_2(x)}{dx} = -D'_{11} \frac{y_2}{b_2} M_2(x) + A'_{11} \frac{N_2(x)}{b_2} - \frac{5t_2}{12G_2} \frac{d\tau_a}{dx} \quad (5d)$$

Where $u_1(x)$ and $u_2(x)$ are the horizontal displacements of the concrete beam and the composite plate respectively. $M_1(x)$ and $M_2(x)$ are respectively the bending moments applied to the concrete beam and the composite plate; E_1 is the Young's modulus of concrete; I_1 the moment of inertia, N_1 and N_2 are the axial forces applied to the concrete and the composite plate respectively, b_1 and t_1 are the width and thickness of the reinforcement plate, $[A'] = [A^{-1}]$ is the inverse of the membrane matrix $[A]$, $[D'] = [D^{-1}]$ is the inverse of the bending matrix.

By writing the conditions of equilibrium of the member 1 (concrete), we will have

In the x direction:

$$\frac{dN_1(x)}{dx} = -b_1 \tau(x) \quad (6a)$$

Where $\tau(x)$ is the shear stress in the adhesive layer.

In the y direction:

$$\frac{dV_1(x)}{dx} = -(\sigma_n(x)b_1 + qb_1) \quad (6b)$$

Where $V_1(x)$ the shear force of the concrete beam is, $\sigma(x)$ is the normal stress at the adhesive layer, q is the distributed load and b_1 the width of the concrete beam.

The moment of balance:

$$\frac{dM_1(x)}{dx} = V_1(x) - b_1 y_1 \tau(x) \quad (7a)$$

The balance of the FRP reinforcement plate in the x and y directions, as well as the moment of equilibrium are written as follows

In the x direction:

$$\frac{dN_2(x)}{dx} = b_2\tau(x) \quad (7b)$$

In the y direction:

$$\frac{dV_2(x)}{dx} = \sigma_n(x)b_2 \quad (7c)$$

The moment of balance:

$$\frac{dM_2(x)}{dx} = V_2(x) - b_2y_2\tau(x) \quad (8)$$

Where $V_2(x)$ is the shear force of the reinforcement plate.

In what follows, the stiffness of the reinforcement plate is significantly lower than that of the concrete beam to be reinforced. The bending moment in the composite plate can be neglected to simplify the shear stress derivation operations.

For the classic laminates (fiber - matrix):

On the other hand, the laminate theory is used to determine the stress and strain of the externally bonded composite plate in order to investigate the whole mechanical performance of the composite strengthened structure. The effective modules of the composite laminate are varied by the orientation of the fibre directions and arrangements of the laminate patterns. The classical laminate theory is used to estimate the strain of the composite plate, i.e.

$$\begin{Bmatrix} \varepsilon^0 \\ k \end{Bmatrix} = \begin{bmatrix} A' & B' \\ C' & D' \end{bmatrix} \begin{Bmatrix} N \\ M \end{Bmatrix} \quad (9a)$$

$$\begin{aligned} [A'] &= [A]^{-1} + [A]^{-1}[B][D^*]^{-1}[B][A]^{-1} \\ [B'] &= -[A]^{-1}[B][D^*]^{-1} \\ [C'] &= [B']^T \\ [D'] &= [D^*]^{-1} \\ [D^*] &= [D] - [B][A]^{-1}[B] \end{aligned} \quad (9b)$$

The terms of the matrices $[A]$, $[B]$ and $[D]$ are written as

Extensional matrix:

$$A_{ij} = \sum_{k=1}^{NN} \bar{Q}_{ij}^k ((y_2)_k - (y_2)_{k-1}) \quad (10a)$$

Extensional–bending coupled matrix:

$$B_{ij} = \frac{1}{2} \sum_{k=1}^{NN} \bar{Q}_{ij}^k ((y_2^2)_k - (y_2^2)_{k-1}) \quad (10b)$$

Flexural matrix:

$$D_{ij} = \frac{1}{3} \sum_{k=1}^{NN} \bar{Q}_{ij}^k ((y_2^3)_k - (y_2^3)_{k-1}) \quad (10c)$$

The subscript NN represents the number of laminate layers of the FRP plate, \bar{Q}_{ij} can be estimated by using the off-axis orthotropic plate theory, where

$$\bar{Q}_{11} = Q_{11}m^4 + 2(Q_{12} + 2Q_{33})m^2n^2 + Q_{22}n^4 \quad (11a)$$

$$\bar{Q}_{12} = (Q_{11} + Q_{22} - 4Q_{33})m^2n^2 + Q_{12}(n^4 + m^4) \quad (11b)$$

$$\bar{Q}_{22} = Q_{11}n^4 + 2(Q_{12} + 2Q_{33})m^2n^2 + Q_{22}m^4 \quad (11c)$$

$$\bar{Q}_{33} = (Q_{11} + Q_{22} - 2Q_{12} - 2Q_{33})m^2n^2 + Q_{33}(n^4 + m^4) \quad (11d)$$

And

$$Q_{11} = \frac{E_1}{1 - \nu_{12}\nu_{21}} \quad (12a)$$

$$Q_{22} = \frac{E_2}{1 - \nu_{12}\nu_{21}} \quad (12b)$$

$$Q_{12} = \frac{\nu_{12}E_2}{1 - \nu_{12}\nu_{21}} = \frac{\nu_{21}E_1}{1 - \nu_{12}\nu_{21}} \quad (12c)$$

$$Q_{33} = G_{12} \quad (12d)$$

$$m = \cos(\theta_j) \quad n = \sin(\theta_j) \quad (12e)$$

Where j is number of the layer; h , \bar{Q}_{ij} and θ_j are respectively the thickness, the Hooke's elastic tensor and the fibers orientation of each layer.

For the Functionally Graded Materials "FGM":

In this study, we consider an imperfect FGM plate with a volume fraction of porosity δ ($\delta \ll 1$), with different form of distribution between the metal and the ceramic. The modified mixture rule proposed by (Hadj *et al.* 2019) and (Rabia *et al.* 2018) is

$$P = P_m \left(V_m - \frac{\alpha}{2} \right) + P_c \left(\left(\frac{z}{h} + \frac{1}{2} \right)^k - \frac{\alpha}{2} \right) \quad (13a)$$

The modified mixture rule becomes

$$P = (P_c - P_m) \left(\frac{z}{h} + \frac{1}{2} \right)^k + P_m - (P_c + P_m) \frac{\alpha}{2} \quad (13b)$$

Where, k is the power law index that takes values greater than or equals to zero. The FGM plate becomes a fully ceramic plate when k is set to zero and fully metal for large value of k . The Young's modulus (E) of the imperfect FG plate can be written as a functions of thickness coordinate, z (middle surface). The material properties of a perfect FGM plate can be obtained when the volume fraction of porosity α is set to zero. Due to the small variations of the Poisson ratio ν , it is assumed to be constant. Several forms of porosity have been studied in the present work, such as uniform distribution "O", "X", "V" and Inverted "V" as follows (Hadj *et al.* 2019), including the deferent's distribution forms of porosity which come in the forms below:

- Uniform distribution shape of the porosity

$$E_2(z) = (e_c - e_m) \times \left(\left(\frac{z}{t_2} + 0.5 \right) \right)^k + e_m - (e_c + e_m) \times \frac{\alpha}{2} \quad (14a)$$

- Form "X" distribution shape of the porosity

$$E_2(z) = (e_c - e_m) \times \left(\left(\frac{z}{t_2} + 0.5 \right) \right)^k + e_m - (e_c + e_m) \times \frac{\alpha}{2} \times \left(2 \times \frac{z}{t_2} \right) \quad (14b)$$

- Form "O" distribution shape of the porosity

$$E_2(z) = (e_c - e_m) \times \left(\left(\frac{z}{t_2} + 0.5 \right) \right)^k + e_m - (e_c + e_m) \times \frac{\alpha}{2} \times \left(1 - 2 \times \frac{|z|}{t_2} \right) \quad (14c)$$

- Form "V" distribution shape of the porosity

$$E_2(z) = (e_c - e_m) \times \left(\left(\frac{z}{t_2} + 0.5 \right) \right)^k + e_m - (e_c + e_m) \times \frac{\alpha}{2} \times \left(\frac{1}{2} + \frac{z}{t_2} \right) \quad (14d)$$

- Inverted Form "V" distribution shape of the porosity

$$E_2(z) = (e_c - e_m) \times \left(\left(\frac{z}{t_2} + 0.5 \right) \right)^k + e_m - (e_c + e_m) \times \frac{\alpha}{2} \times \left(\frac{1}{2} - \frac{z}{t_2} \right) \quad (14e)$$

Being given that $E_2(z)$ is determined according to the form of distribution of the porosity in the imperfect FGM plate, given by the Eqs. (9), (7), (8), (9) and (10), the linear constitutive relations of a FGM plate can be written as

$$\begin{aligned} Q_{11} &= Q_{22} = \frac{E_2(z)}{1 - \nu^2} \\ Q_{12} &= \frac{\nu E_2(z)}{1 - \nu^2} \\ Q_{33} &= \frac{E_2(z)}{2(1 + \nu)} \end{aligned} \quad (15)$$

where $(\sigma_x, \sigma_y, \tau_{xy}, \tau_{yz}, \tau_{yx})$ and $(\varepsilon_x, \varepsilon_y, \gamma_{xy}, \gamma_{yz}, \gamma_{yx})$ are the stress and strain components, respectively, and A_{ij}, D_{ij} are the plate stiffness, defined by

$$A_{ij} = \int_{-h/2}^{h/2} Q_{ij}z \quad D_{ij} = \int_{-h/2}^{h/2} Q_{ij}z^2 dz \quad (16)$$

where A'_{11} , D'_{11} are defined as

$$A'_{11} = \frac{A_{22}}{A_{11}A_{22} - A_{12}^2} \quad D'_{11} = \frac{D_{22}}{D_{11}D_{22} - D_{12}^2} \quad (17)$$

2.3 Mathematical formulation of the present model:

Shear stress distribution along the composite–damaged concrete interface

The governing differential equation for the interfacial shear stress is expressed as Daouadji *et al.* (2016b)

$$\begin{aligned} \frac{d^2\tau(x)}{dx^2} - \frac{A'_{11} + \frac{b_2}{\bar{E}_{11}A_1} + \frac{(y_1 + y_2)(y_1 + y_2 + t_a)}{\bar{E}_{11}I_1D'_{11} + b_2} b_2D'_{11}}{\frac{t_a}{G_a} + \frac{t_2}{3G_2}} \tau(x) \\ + \frac{\frac{(y_1 + y_2)}{\bar{E}_{11}I_1D'_{11} + b_2} D'_{11}}{\frac{t_a}{G_a} + \frac{t_2}{3G_2}} V_T(x) = 0 \end{aligned} \quad (18)$$

$$K_1 = \frac{1}{\frac{t_a}{G_a} + \frac{t_2}{3G_2}} \quad (19)$$

For simplicity, the general solutions presented below are limited to loading which is either concentrated or uniformly distributed over part or the whole span of the beam, or both. For such loading, $d^2V_T(x)/dx^2 = 0$, and the general solution to Eq. (18) is given by

$$\tau(x) = \xi_1 \cos h(\delta x) + \xi_2 \sin h(\delta x) + \rho V_T(x) \quad (20a)$$

$$\begin{aligned} \tau(x) = \xi_1 \cos h(\delta x) + \xi_2 \sin h(\delta x) \\ + \frac{\frac{(y_1 + t_2/2)}{\bar{E}_{11}I_1D'_{11} + b_2} D'_{11}}{A'_{11} + \frac{b_2}{\bar{E}_{11}A_1} + \frac{(y_1 + t_2/2)(y_1 + t_a + t_2/2)}{\bar{E}_{11}I_1D'_{11} + b_2} b_2D'_{11}} V_T(x) \end{aligned} \quad (20b)$$

Where

$$\delta = \sqrt{\frac{A'_{11} + \frac{b_2}{\bar{E}_{11}A_1} + \frac{(y_1 + t_2/2)(y_1 + t_a + t_2/2)}{\bar{E}_{11}I_1D'_{11} + b_2} b_2D'_{11}}{\frac{t_a}{G_a} + \frac{t_2}{3G_2}}} \quad (21a)$$

$$\rho = \frac{\frac{(y_1 + t_2/2)}{\bar{E}_{11}I_1D'_{11} + b_2} D'_{11}}{A'_{11} + \frac{b_2}{\bar{E}_{11}A_1} + \frac{(y_1 + t_2/2)(y_1 + t_a + t_2/2)}{\bar{E}_{11}I_1D'_{11} + b_2} b_2 D'_{11}} \quad (21b)$$

And ξ_1 and ξ_2 are constant coefficients determined from the boundary conditions. In the present study, a simply supported beam has been investigated which is subjected to a uniformly distributed load (Fig. 3). The interfacial shear stress for this uniformly distributed load at any point is written as Daouadji *et al.* (2016b)

$$\tau(x) = \left[\frac{\frac{a \cdot y_1}{2}}{\bar{E}_1 I_1 \left(\frac{t_a}{G_a} + \frac{t_1}{4G_1} \right)} (l - a) - \frac{\frac{y_1 + 0,5t_2}{\bar{E}_1 I_1 D'_{11} + b_2} D'_{11}}{\left(\frac{t_a}{G_a} + \frac{t_1}{4G_1} \right) \delta^2} \right] \frac{q e^{-\delta x}}{\delta} + \frac{\frac{y_1 + 0,5t_2}{\bar{E}_1 I_1 D'_{11} + b_2} D'_{11}}{\delta^2 \left(\frac{t_a}{G_a} + \frac{t_1}{4G_1} \right)} q \left(\frac{l}{2} - a - x \right) \quad (22)$$

Where q is the uniformly distributed load and x ; a ; l and l_p are defined in Fig. 2.

2.4 Mathematical formulation of the present model: Interfacial normal stress distribution along the composite–damaged concrete interface

The following governing differential equation for the interfacial normal stress (Daouadji *et al.* 2016b)

$$\frac{d^4 \sigma_n(x)}{dx^4} + K_n \left(D'_{11} + \frac{b_2}{\bar{E}_1 I_1} \right) \sigma_n(x) - K_n \left(D'_{11} \frac{t_2}{2} - \frac{y_1 b_2}{\bar{E}_1 I_1} \right) \frac{d\tau(x)}{dx} + \frac{q K_n}{\bar{E}_1 I_1} = 0 \quad (23)$$

The general solution to this fourth–order differential equation is

$$\sigma_n(x) = e^{-\eta x} [\xi_3 \cos(\eta x) + \xi_4 \sin(\eta x)] + e^{\eta x} [\xi_5 \cos(\eta x) + \xi_6 \sin(\eta x)] - \gamma_1 \frac{d\tau(x)}{dx} - \frac{q}{D'_{11} \bar{E}_1 I_1 + b_2} \quad (24)$$

For large values of x it is assumed that the normal stress approaches zero and, as a result, $\xi_5 = \xi_6 = 0$. The general solution therefore becomes

$$\sigma_n(x) = e^{-\eta x} [\xi_3 \cos(\eta x) + \xi_4 \sin(\eta x)] - \gamma_1 \frac{d\tau(x)}{dx} - \frac{q}{D'_{11} \bar{E}_1 I_1 + b_2} \quad (25)$$

Where

$$\eta = \sqrt[4]{\frac{K_n}{4} \left(D'_{11} + \frac{b_2}{\bar{E}_1 I_1} \right)} \quad (26a)$$

$$\gamma_1 = \frac{y_1 b_2 - 0,5(D'_{11} \bar{E}_1 I_1 t_2)}{D'_{11} \bar{E}_1 I_1 + b_2} \quad (26b)$$

As is described by Daouadji *et al.* (2016a), the constants ξ_3 and ξ_4 in Eq. (23) are determined using the appropriate boundary conditions and they are written as follows

$$\xi_3 = \frac{K_n}{2\eta^3 E_1 I_1} [V_T(0) + \eta M_T(0)] - \frac{\gamma_2}{2\eta^3} \tau(0) + \frac{\gamma_1}{2\eta^3} \left(\frac{d^4 \tau(0)}{dx^4} + \eta \frac{d^3 \tau(0)}{dx^3} \right) \quad (26c)$$

$$\xi_4 = -\frac{K_n}{2\eta^2 E_1 I_1} M_T(0) - \frac{\gamma_1}{2\eta^2} \frac{d^3 \tau(0)}{dx^3} \quad (26d)$$

$$\gamma_2 = b_2 K_n \left(\frac{y_1}{E_1 I_1} - \frac{D'_{11} t_2}{2b_2} \right) \quad (26e)$$

The above expressions for the constants B_3 and B_4 has been left in terms of the bending moment $M_T(0)$ and shear force $V_T(0)$ at the end of the soffit plate. With the constants ξ_3 and ξ_4 determined, the interfacial normal stress can then be found using Eq. (23).

3. Numerical results and discussions

3.1 Material used

The material used for the present studies is an damaged porous RC cantilever beam bonded with different type of composite materials plate (GFRP, CFRP, Sika Carbodur, Sika Wrap and FGM). A summary of the geometric and material properties is given in Table 1 and Fig. 3. The span of the damaged porous RC cantilever beam is 1500 mm, the distance from the support to the end of the plate is 500 mm and the uniformly distributed load is 30 kN/m.

3.2 Comparison with analytical solutions

A comparison of the interfacial shear and normal stresses from the different existing closed-form solutions and the present new solution is undertaken in this section. An undamaged RC beam bonded with a CFRP soffit plate is considered. Fig. 4 plots the interfacial shear and normal stresses near the plate end for the example RC cantilever beam bonded with a CFRP plate for the uniformly distributed load case.

The present analysis gives lower maximum interfacial shear and normal stresses than those predicted by Daouadji *et al.* (2016b), indicating that the inclusion of adherend shear deformation effect in the beam and soffit plate leads to lower values of τ_{max} and σ_{max} . However, the maximum interfacial shear and normal stresses given by He *et al.* (2019) are lower than the results computed by the present solution. This difference is due to the assumption used in the present theory which is in agreement with the beam theory (parabolic distribution of shear stresses through the depth of the beam). Hence, it is apparent that the adherend shear deformation reduces the interfacial stresses concentration and thus renders the adhesive shear distribution more uniform. The interfacial normal

Table 1 Mechanical properties of the materials used

Component	Young's modulus (MPa)	Poisson's ratio
Reinforced concrete	$E_1 = 30000$	0.18
Adhesive layer	$E_a = 6700$	0.4
Sika Carbodur strengthening plate	$E_2 = 165\ 000$	0.3
Sika Wrap strengthening plate	$E_2 = 230\ 000$	0.3
CFRP strengthening plate	$E_2 = 140\ 000$	0.28
GFRP strengthening plate	$E_2 = 50\ 000$	0.28
FGM strengthening plate	$E_{ceramic} = 380\ 000$ $E_{metal} = 70\ 000$	0.3

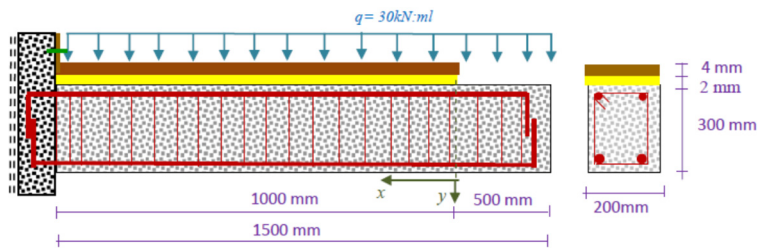


Fig. 3 Geometric characteristic of a damaged porous RC cantilever beam strengthening with composite plate

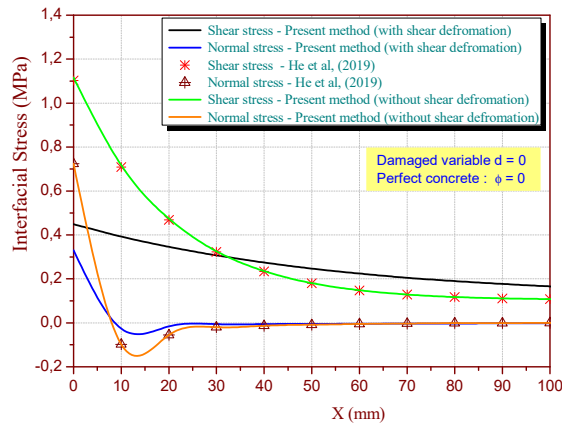


Fig. 4 Comparison of interfacial shear and normal stresses for an RC cantilever beam with a bonded CFRP plate subjected to a uniformly distributed load

stress is seen to change sign at a short distance away from the plate end. Overall, the predictions of the different solutions agree closely with the results He *et al.* (2019).

3.3 Effect of the variation of the damage variable on the interfacial stresses

The analysis of the effect of the variation of the damage variable on the interfacial stresses of the damaged porous RC cantilever beam enhanced with a composite plate (Tables 2 and 3, Figs. 5 and

Table 2 Effect of the variation of the damage variable on the interfacial shear stress of the porous RC cantilever beam strengthened with a composite plate

Porosity of concrete “ ϕ ”	Damage variable “ d ”	Damage RC cantilever beam strengthened with				
		CFRP	GFRP	Sika Wrap	Sika Carbodur	Perfect FGM $k = 10$
		$\tau(x)$ MPa	$\tau(x)$ MPa	$\tau(x)$ MPa	$\tau(x)$ MPa	$\tau(x)$ MPa
$\phi = 0$	0,0	0,44865	0,25360	0,40338	0,49078	0,50381
	0,1	0,47735	0,27008	0,42938	0,52190	0,53564
	0,2	0,51113	0,28960	0,46006	0,55843	0,57300
	0,3	0,55165	0,31324	0,49696	0,60211	0,61761
$\phi = 0,01$	0,0	0,45133	0,25514	0,40580	0,49369	0,50678
	0,1	0,48016	0,27170	0,43193	0,52494	0,53876
	0,2	0,51410	0,29133	0,46276	0,56164	0,57627
	0,3	0,55480	0,31509	0,49983	0,60550	0,62107
$\phi = 0,02$	0,0	0,45404	0,25669	0,40826	0,49664	0,50980
	0,1	0,48302	0,27334	0,43452	0,52803	0,54192
	0,2	0,51711	0,29307	0,46550	0,56489	0,57959
	0,3	0,55798	0,31696	0,50274	0,60893	0,62457
$\phi = 0,03$	0,0	0,45680	0,25827	0,41076	0,49963	0,51286
	0,1	0,48591	0,27501	0,43715	0,53117	0,54513
	0,2	0,52017	0,29485	0,46828	0,56818	0,58296
	0,3	0,56123	0,31887	0,50570	0,61241	0,62813

Table 3 Effect of the variation of the damage variable on the interfacial normal stress of the porous RC cantilever beam strengthened with a composite plate

Porosity of concrete “ ϕ ”	Damage variable “ d ”	Damage RC cantilever beam strengthened with				
		CFRP	GFRP	Sika Wrap	Sika Carbodur	Perfect FGM $k = 10$
		$\sigma_i(x)$ MPa	$\sigma_i(x)$ MPa	$\sigma_i(x)$ MPa	$\sigma_n(x)$ MPa	$\sigma_n(x)$ MPa
$\phi = 0$	0,0	0,33034	0,23700	0,43260	0,34785	0,34432
	0,1	0,35275	0,25342	0,46141	0,37124	0,36747
	0,2	0,37926	0,27295	0,49547	0,39885	0,39480
	0,3	0,41125	0,29671	0,53654	0,43206	0,42766
$\phi = 0,01$	0,0	0,33243	0,23853	0,43528	0,35003	0,34648
	0,1	0,35495	0,25503	0,46424	0,37353	0,36975
	0,2	0,38160	0,27468	0,49847	0,40128	0,39720
	0,3	0,41374	0,29858	0,53974	0,43465	0,43022

Table 3 Continued

Porosity of concrete “ ϕ ”	Damage variable “ d ”	Damage RC cantilever beam strengthened with				
		CFRP	GFRP	Sika Wrap	Sika Carbodur	Perfect FGM $k = 10$
		$\sigma_i(x)$ MPa	$\sigma_i(x)$ MPa	$\sigma_i(x)$ MPa	$\sigma_i(x)$ MPa	$\sigma_i(x)$ MPa
$\phi = 0,02$	0,0	0,33454	0,24008	0,43800	0,35224	0,34867
	0,1	0,35719	0,25667	0,46711	0,37586	0,37205
	0,2	0,38397	0,27643	0,50152	0,40374	0,39964
	0,3	0,41627	0,30047	0,54299	0,43727	0,43281
$\phi = 0,03$	0,0	0,33670	0,24165	0,44077	0,35449	0,35089
	0,1	0,35946	0,25834	0,47003	0,37823	0,37439
	0,2	0,38638	0,27821	0,50461	0,40624	0,40212
	0,3	0,41884	0,30239	0,54629	0,43993	0,43544

6), We noted that more the variable of damage increases more the interface stresses become important in other words that more the rigidity of the damaged porous RC cantilever beam decreases more we recorded more important stresses where the peeling off of the strengthening composite plate approaches, also the less rigid the reinforcement plates (in order from least rigid to most rigid: from GFRP, sika wrap, CFRP, sika carbodur and FGM) the more the stresses become low, object of our research since we aim to decrease these values of the stresses; to ensure proper strengthening of the plate.

Figs. 5 and 6 show the effect of damage extent on maximum shear and normal interfacial stresses, respectively, for the five types of GFRP, sika wrap, CFRP, sika carbodur and FGM materials. The results show that when the damage variable increases from 0 to 0.3; the maximum interfacial stress increases slowly. This analysis of the variable damage effect is identical to the effect of the porosity of concrete.

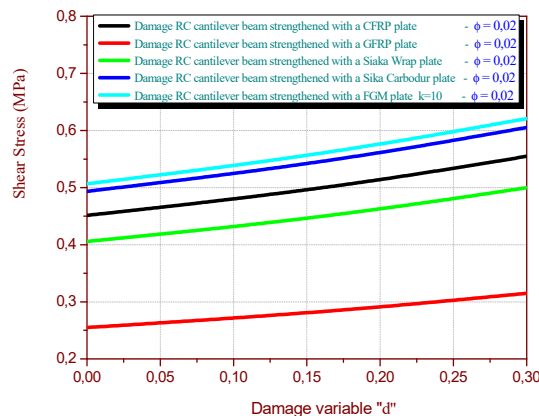


Fig. 5 Effect of the variation of the damage variable on the interfacial shear stress of the porous RC cantilever beam strengthened with a composite

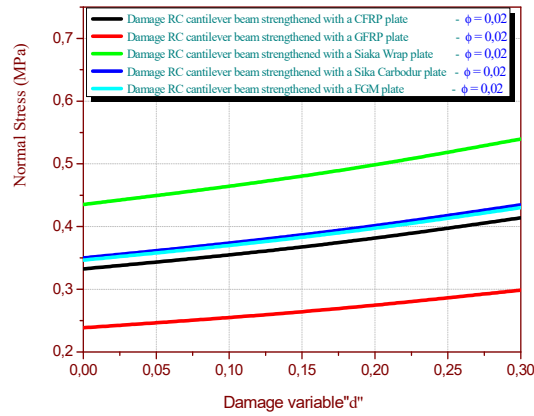


Fig. 6 Effect of the variation of the damage variable on the interfacial normal stress of the porous RC cantilever beam strengthened with a composite

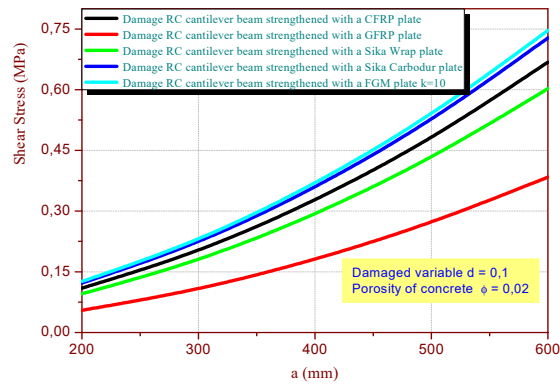


Fig. 7 Effect of length of unstrengthened on interfacial shear stress in damaged porous RC cantilever beam strengthened with a composite

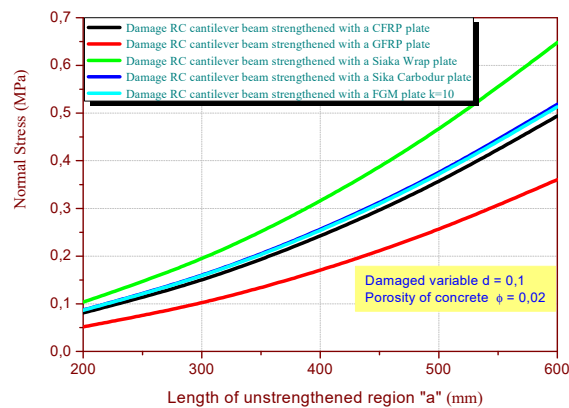


Fig. 8 Effect of length of unstrengthened on interfacial normal stress in damaged porous RC cantilever beam strengthened with a composite

3.4 Effect of length of unstrengthened region "a"

The influence of the length of the ordinary-beam region (the region between the support and the end of the composite strip on the edge stresses) appears in Figs. 7 and 8 of a damaged porous RC cantilever beam strengthened with a composite plate. It is seen that, as the plate terminates further from the free edge, the interfacial stresses increase significantly.

This result reveals that in any case of strengthening, including cases where retrofitting is required in a limited zone of maximum bending moments at midspan, it is recommended to extend the strengthening strip as possible to the length of the beam.

3.5 Effect of the thickness of the adhesive layer

Figs. 9 and 10, show the effect of the thickness of the adhesive layer affects only the concentrations of interfacial stresses, hardly the stress levels. However, design of the properties and

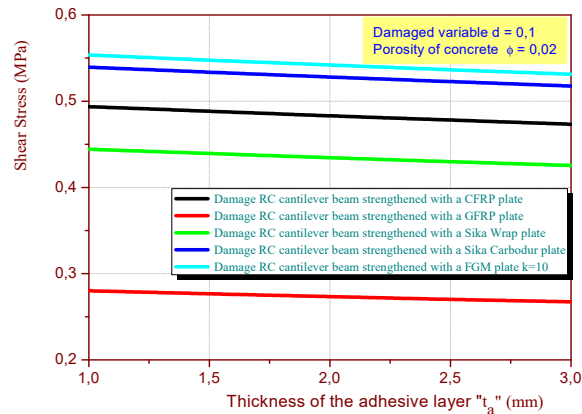


Fig. 9 Effect of thickness of the adhesive layer on interfacial shear stress in damaged porous RC cantilever beam strengthened with a composite plate

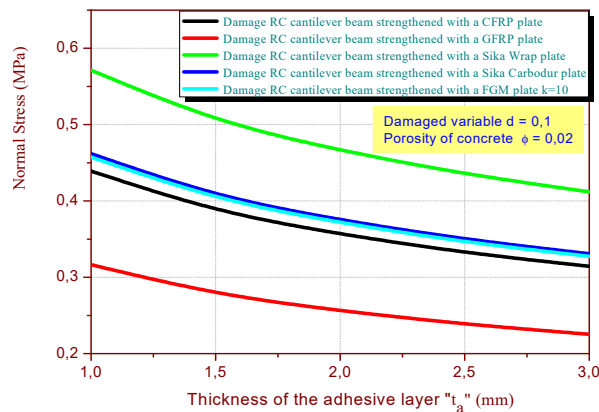


Fig. 10 Effect of Thickness of the adhesive layer on interfacial normal stress in damaged porous RC cantilever beam strengthened with a composite plate

thickness of the adhesive is a difficult problem, in particular on the structures in service concerned by the rehabilitation (a real case will be presented later). An optimization design of the adhesive is expected, this is one of our perspectives soon.

3.6 Effect of fibers orientation for CFRP plate

The effect of fiber orientation on adhesive stresses is show in Figs. 11 and 12 of a damaged porous RC cantilever beam strengthened with a CFRP plate, the maximum interfacial stresses (shear and normal) increase with increasing alignment of all high strength fibers in the composite plate in beam's longitudinal direction x . In order to minimize the concentration of stresses at the free edge of the beam, it is very logical to adopt CFRP with fibers perpendicular to 0) (i.e., $\theta = 90^\circ$).

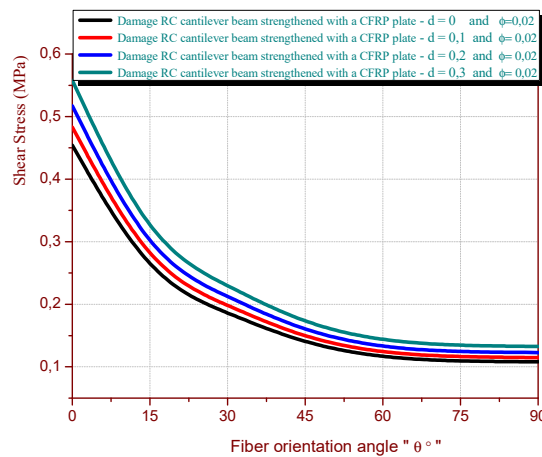


Fig. 11 Effect of fibers orientation on interfacial shear stress in damaged porous RC cantilever beam strengthened with a CFRP

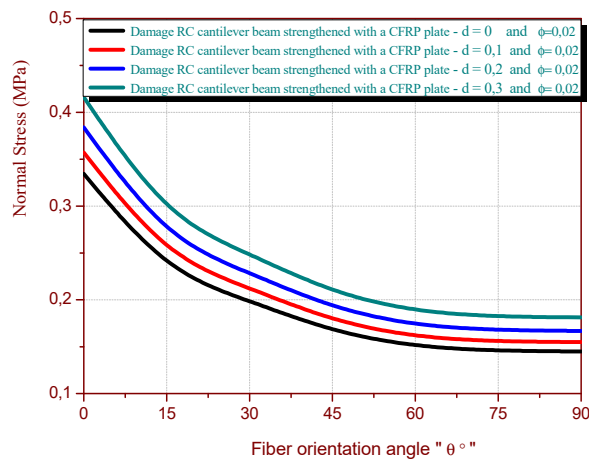


Fig. 12 Effect of fibers orientation on interfacial normal stress in damaged porous RC cantilever beam strengthened with a CFRP

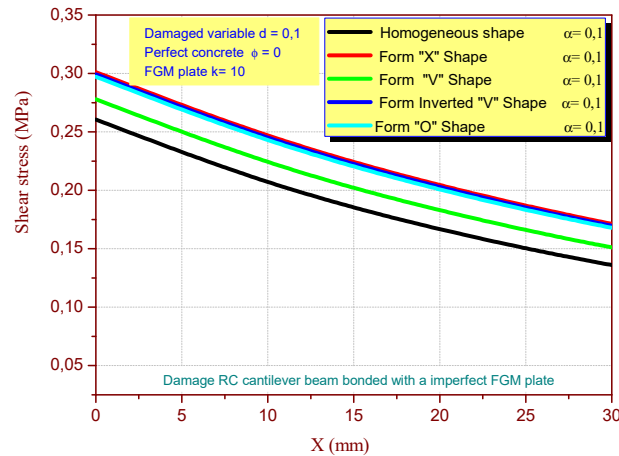


Fig. 13 Effect of distribution forms of porosity on interfacial shear stress in damaged porous RC cantilever beam strengthened with a FGM

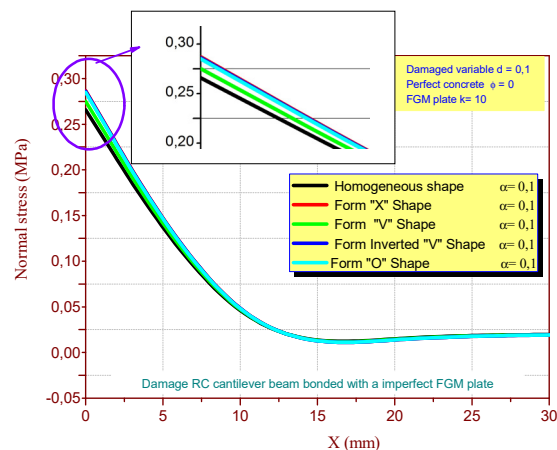
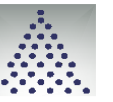


Fig. 14 Effect of distribution forms porosity on interfacial normal stress in damaged porous RC cantilever beam strengthened with a FGM

3.7 Effect of distribution forms of porosity from FGM materials

Table 6 and Figs. 13 and 14 clearly show the effect of the variation of the distribution forms of porosity on the interfacial stress (shear and normal) of the damaged porous RC cantilever beam strengthened with a porous FGM plate under uniform distributed load, which demonstrate the effect of material properties on shear stress. Taking into account the variation in the forms of porosity distribution and the index of this porosity (from $\alpha = 0,05$ to $\alpha = 0,2$) (Fig. 15). The results show that, as the material becomes softer (from the least porous material $a = 0,05$ to the most porous material $a = 0,2$), the shear stress interface becomes smaller, unexpected. same load, the reinforced resistance developed in the smaller plate, which made it possible to reduce the interfacial stresses. interfacial shear peak plate becomes less stiff.

Table 6 Effect of the porosity index of the FGM plate according to the forms of distribution on the interfacial stress of a damaged porous RC cantilever beam reinforced with a porous FGM plate

Index of porosity of FGM plate " α "	Distribution forms of porosity				
	Homogeneous shape	Form "X" Shape	Form "O" Shape	Form "V" Shape	Form Inverted "V" Shape
					
Shear Stress (MPa)					
Value of other parameters: $d = 0$; $\phi = 0$ and FGM - $k = 10$					
0	0,3129	0,3129	0,3129	0,3129	0,3129
0,05	0,2871	0,3058	0,2989	0,2958	0,3051
0,1	0,2606	0,3012	0,2971	0,2780	0,2992
0,15	0,2349	0,2989	0,2989	0,2595	0,2960
0,2	0,2155	0,2989	0,2989	0,2402	0,2971
Normal Stress (MPa)					
Value of other parameters: $d = 0$; $\phi = 0$ and FGM - $k = 10$					
0	0,2679	0,2679	0,2679	0,2679	0,2679
0,05	0,2511	0,2644	0,2609	0,2593	0,2640
0,1	0,2408	0,2620	0,2600	0,2501	0,2610
0,15	0,2266	0,2609	0,2609	0,2402	0,2594
0,2	0,2155	0,2609	0,2609	0,2296	0,2600

It is pointed out that, for the X-shaped forms of porosity distribution where the pores are concentrated on the upper and lower face of the beam, in this case the FGM plate of reinforcement of the beam becomes in these parts weak and consequently the interface constraints increase

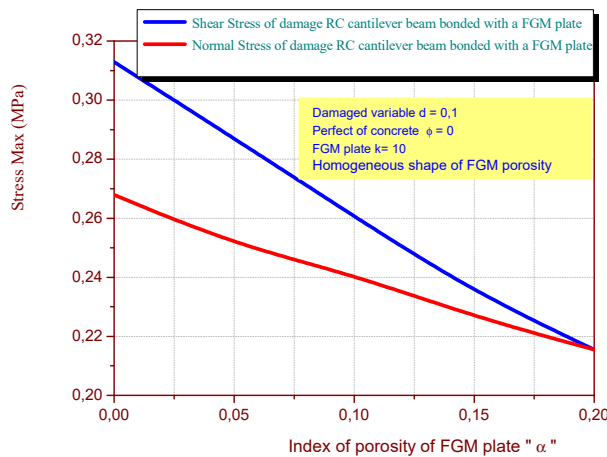


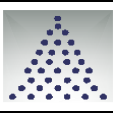
Fig. 15 Effect of porosity index on interfacial stress in damaged porous RC cantilever beam strengthened with a FGM plate

compared to other modes of porosity distribution.

3.8 Effect of the FGM plate stiffness “index – k ”

Table 7 represent the interfacial shear stress distributions in the example in a damaged porous Rc cantilever beam strengthened with imperfect FGM plate under uniform distributed load. For this problem, the rigidity of the soffit plate is of much greater significance than in the RC cantilever beam problem. The effects of bending deformations in the plate and axial deformations in the beam are therefore expected to become significant. The study consists in varying the FGM from ceramic ($k = 0$) to metal ($k = \infty$) while varying the material FGM for $k = 0 - 2,5 - 5 - 7,5 - 10$ and $k = 20$ as an example it's just to see the effect stiffness of the reinforcement plate (case of Table 4), also a variation of the homogeneity index of the FGM (index k); from the least rigid FGM to the most rigid FGM was presented. The results show that, as the plate material becomes softer (from ceramic, FGM (different value of the index k) to metal), the interfacial shear stress become smaller, as expected. This is because, under the same load, the tensile force developed in the plate is smaller, which leads to reduced shear stresses. The position of the peak interfacial shear stress moves closer to the free edge as the plate becomes softer.

Table 7 Effect of the FGM plate stiffness (index - k) on the interfacial stress of a damaged porous RC cantilever beam reinforced with a porous FGM plate

Degree of homogeneity of the FGM material “ k ”	Distribution forms of porosity				
	Homogeneous shape	Form “X” Shape	Form “O” Shape	Form “V” Shape	Form Inverted “V” Shape
					
Shear stress (MPa)					
Value of other parameters: $d = 0$; $\phi = 0$ and $\alpha = 0,1$					
0	0,7362	0,7595	0,7367	0,7479	0,7479
2,5	0,4923	0,4862	0,5260	0,4867	0,5155
5	0,3620	0,3589	0,4109	0,3551	0,3919
7,5	0,2898	0,3120	0,3358	0,2961	0,3258
10	0,2606	0,3012	0,2971	0,2780	0,2992
20	0,2480	0,3012	0,2691	0,2747	0,2854
Normal stress (MPa)					
Value of other parameters: $d = 0$; $\phi = 0$ and $\alpha = 0,1$					
0	0,6476	0,6681	0,6481	0,6579	0,6579
2,5	0,4322	0,4269	0,4621	0,4273	0,4528
5	0,3172	0,3145	0,3604	0,3111	0,3436
7,5	0,2535	0,2731	0,2941	0,2591	0,2853
10	0,2408	0,2620	0,2600	0,2501	0,2610
20	0,2166	0,2635	0,2352	0,2402	0,2496

4. Conclusions

This research has been concerned with the prediction of interfacial shear and normal stresses in damaged porous RC cantilever beams retrofitted with externally advanced composite materials. Such interfacial stresses provide the basis for understanding debonding failures in such beams and for development of suitable design rules. Analytical comparison between the existing solutions and the present new solution has been carried out. The isotropic damage model is adopted to describe the damage of the RC cantilever beams as well as manufacturing defects in concrete. The results show that the damage concrete manufacturing defects and the porosity of FGM materials has a significant effect on the interfacial stresses in composite-damaged porous RC cantilever beam, especially, when the length of damaged region is equal or superior to the plate length. Therefore, it is recommended to use a perfect thin reinforcement plate with a length greater than that of the damaged area for perfect concrete too and preferably to extend the reinforcement plate along the cantilever beam. The results reveal also that the thickness of the composite strip significantly increases the edge peeling and shear stresses.

Acknowledgments

This research was supported by the Algerian Ministry of Higher Education and Scientific Research (MESRS) as part of the grant for the PRFU research project n° A01L02UN140120200002 and by the University of Tiaret, in Algeria.

References

- Abdelhak, Z., Hadji, L., Daouadji, T.H. and Adda Bedia, E.A. (2016), "Thermal buckling response of functionally graded sandwich plates with clamped boundary conditions", *Smart Struct. Syst., Int. J.*, **18**(2), 267-291. <https://doi.org/10.12989/sss.2016.18.2.267>
- Abderezak, R., Daouadji, T.H., Rabia, B. and Belkacem, A. (2018a), "Nonlinear analysis of damaged RC beams strengthened with glass fiber reinforced polymer plate under symmetric loads", *Earthq. Struct., Int. J.*, **15**(2), 113-122. <https://doi.org/10.12989/eas.2018.15.2.113>
- Abderezak, R., Daouadji, T.H., Abbes, B., Rabia, B., Belkacem, A. and Abbes, F. (2018b), "Elastic analysis of interfacial stress concentrations in CFRP-RC hybrid beams: Effect of creep and shrinkage", *Adv. Mater. Res., Int. J.*, **6**(3), 257-278. <https://doi.org/10.12989/amr.2017.6.3.257>
- Abderezak, R., Rabia, B., Daouadji, T.H., Abbes, B., Belkacem, A. and Abbes, F. (2019), "Elastic analysis of interfacial stresses in prestressed PFGM-RC hybrid beams", *Adv. Mater. Res., Int. J.*, **7**(2), 83-103. <https://doi.org/10.12989/amr.2018.7.2.083>
- Abderezak, R., Daouadji, T.H. and Rabia, B. (2020), "Analysis of interfacial stresses of the reinforced concrete foundation beams repairing with composite materials plate", *Coupl. Syst. Mech., Int. J.*, **9**(5), 473-498. <http://dx.doi.org/10.12989/csm.2020.9.5.473>
- Abderezak, R., Daouadji, T.H. and Rabia, B. (2021a), "Aluminum beam reinforced by externally bonded composite materials", *Adv. Mater. Res., Int. J.*, **10**(1), 23-44. <http://dx.doi.org/10.12989/amr.2021.10.1.023>
- Abderezak, R., Daouadji, T.H. and Rabia, B. (2021b), "Modeling and analysis of the imperfect FGM-damaged RC hybrid beams", *Adv. Computat. Des., Int. J.*, **6**(2), 117-133. <http://dx.doi.org/10.12989/acd.2021.6.2.117>
- Abualnour, M., Chikh, A., Hebali, H., Kaci, A., Tounsi, A., Bousahla, A.A. and Tounsi, A. (2019), "Thermomechanical analysis of antisymmetric laminated reinforced composite plates using a new four

- variable trigonometric refined plate theory”, *Comput. Concrete, Int. J.*, **24**(6), 489-498.
<https://doi.org/10.12989/cac.2019.24.6.489>
- Adim, B., Daouadji, T.H. and Abbes, B. (2016a), “Buckling analysis of anti-symmetric cross-ply laminated composite plates under different boundary conditions”, *Int. Appl. Mech.*, **52**(6), 126-141.
<https://doi.org/10.1007/s10778-016-0787-x>
- Adim, B., Daouadji, T.H., Abbes, B. and Rabahi, A. (2016b), “Buckling and free vibration analysis of laminated composite plates using an efficient and simple higher order shear deformation theory”, *Mech. Indust.*, **17**, 512. <https://doi.org/10.1051/meca/2015112>
- Adim, B., Daouadji, T.H., Rabia, B. and Hadji, L. (2016c), “An efficient and simple higher order shear deformation theory for bending analysis of composite plates under various boundary conditions”, *Earthq. Struct., Int. J.*, **11**(1), 63-82. <https://doi.org/10.12989/eas.2016.11.1.063>
- Aicha, K., Rabia, B., Daouadji, T.H. and Bouzidene, A. (2020), “Effect of porosity distribution rate for bending analysis of imperfect FGM plates resting on Winkler-Pasternak foundations under various boundary conditions”, *Coupl. Syst. Mech., Int. J.*, **9**(6), 575-597.
<http://dx.doi.org/10.12989/csm.2020.9.6.575>
- AkhavanAlavi, S.M., Mohammadimehr, M. and Edjtahed, S.H. (2019), “Active control of micro Reddy beam integrated with functionally graded nanocomposite sensor and actuator based on linear quadratic regulator method”, *Eur. J. Mech. A/Solids*, **74**, 449-461. <https://doi.org/10.1016/j.euromechsol.2018.12.008>
- Alambeigi, K., Mohammadimehr, M., Bamdad, M. and Rabczuk, T. (2020), “Free and forced vibration analysis of a sandwich beam considering porous core and SMA hybrid composite face layers on Vlasov’s foundation”, *Acta Mechanica*, Article 231, 3199-3218. <https://doi.org/10.1007/s00707-020-02697-5>
- Alimirzaei, S., Mohammadimehr, M. and Tounsi, A. (2019), “Nonlinear analysis of viscoelastic micro-composite beam with geometrical imperfection using FEM: MSGT electro-magneto-elastic bending, buckling and vibration solutions”, *Struct. Eng. Mech., Int. J.*, **71**(5), 485-502.
<https://doi.org/10.12989/sem.2019.71.5.485>
- Antar, K., Amara, K., Benyoucef, S., Bouazza, M. and Ellali, M. (2019), “Hygrothermal effects on the behavior of reinforced-concrete beams strengthened by bonded composite laminate plates”, *Struct. Eng. Mech., Int. J.*, **69**(3), 327-334. <https://doi.org/10.12989/sem.2019.69.3.327>
- Atmane, H.A., Tounsi, A. and Bernard, F. (2015), “Effect of thickness stretching and porosity on mechanical response of a functionally graded beams resting on elastic foundations”, *Int. J. Mech. Mater. Des.*, **13**(1), 71-84. <https://doi.org/10.1007/s10999-015-9318-x>
- Babaeecian, M. and Mohammadimehr, M. (2020), “Investigation of the time elapsed effect on residual stress measurement in a composite plate by DIC method”, *Optics Lasers Eng.*, **128**, 106002.
<https://doi.org/10.1016/j.optlaseng.2020.106002>
- Belkacem, A., Tahar, H.D., Abderrezak, R., Amine, B.M., Mohamed, Z. and Boussad, A. (2018), “Mechanical buckling analysis of hybrid laminated composite plates under different boundary conditions”, *Struct. Eng. Mech., Int. J.*, **66**(6), 761-769. <https://doi.org/10.12989/sem.2018.66.6.761>
- Benferhat, R., Daouadji, T.H., Mansour, M.S. and Hadji, L. (2016a), “Effect of porosity on the bending and free vibration response of functionally graded plates resting on Winkler-Pasternak foundations”, *Earthq. Struct., Int. J.*, **10**(6), 1429-1449. <https://doi.org/10.12989/eas.2016.10.6.1429>
- Benferhat, R., Daouadji, T.H. and Adim, B. (2016b), “A novel higher order shear deformation theory based on the neutral surface concept of FGM plate under transverse load”, *Adv. Mater. Res, Int. J.*, **5**(2), 107-120.
<https://doi.org/10.12989/amr.2016.5.2.107>
- Benferhat, R., Daouadji, T.H. and Mansour, M.S. (2016c), “Free vibration analysis of FG plates resting on the elastic foundation and based on the neutral surface concept using higher order shear deformation theory”, *Comptes Rendus Mecanique*, **344**(9), 631-641. <https://doi.org/10.1016/j.crme.2016.03.002>
- Benferhat, R., Daouadji, T.H. and Abderezak, R. (2021), “Effect of porosity on fundamental frequencies of FGM sandwich plates”, *Compos. Mater. Eng.*, **3**(1), 25-40. <http://dx.doi.org/10.12989/cme.2021.3.1.025>
- Benhenni, M.A., Daouadji, T.H., Abbes, B., Adim, B., Li, Y. and Abbes, F. (2018), “Dynamic analysis for anti-symmetric cross-ply and angle-ply laminates for simply supported thick hybrid rectangular plates” *Adv. Mater. Res., Int. J.*, **7**(2), 83-103. <https://doi.org/10.12989/amr.2018.7.2.119>

- Benhenni, M.A., Daouadji, T.H., Abbes, B., Abbes, F., Li, Y. and Adim, B. (2019), "Numerical analysis for free vibration of hybrid laminated composite plates for different boundary conditions", *Struct. Eng. Mech., Int. J.*, **70**(5), 535-549. <https://doi.org/10.12989/sem.2019.70.5.535>
- Bensattalah, T., Zidour, M. and Daouadji, T.H. (2018), "Analytical analysis for the forced vibration of CNT surrounding elastic medium including thermal effect using nonlocal Euler-Bernoulli theory", *Adv. Mater. Res., Int. J.*, **7**(3), 163-174. <https://doi.org/10.12989/amr.2018.7.3.163>
- Benyoucef, S., Tounsi, A., Meftah, S.A. and Adda-Bedia, E.A. (2007), "Approximate analysis of the interfacial stress concentrations in FRP-RC hybrid beams", *Compos. Interf.*, **13**(7), 561-571. <https://doi.org/10.1163/156855406778440758>
- Bouakaz, K., Daouadji, T.H., Meftah, S.A., Ameer, M., Tounsi, A. and Bedia, E.A. (2014), "A numerical analysis of steel beams strengthened with composite materials", *Mech. Compos. Mater.*, **50**(4), 685-696. <https://doi.org/10.1007/s11029-014-9435-x>
- Boulal, A., Bensattalah, T., Karas, A., Zidour, M., Heireche, H. and Adda Bedia, E.A. (2020), "Buckling of carbon nanotube reinforced composite plates supported by Kerr foundation using Hamilton's energy principle", *Struct. Eng. Mech., Int. J.*, **73**(2), 209-223. <https://doi.org/10.12989/sem.2020.9.73.209>
- Chedad, A., Daouadji, T.H., Abderezak, R., Belkacem, A., Abbes, B., Rabia, B. and Abbes, F. (2018), "A high-order closed-form solution for interfacial stresses in externally sandwich FGM plated RC beams", *Adv. Mater. Res., Int. J.*, **6**(4), 317-328. <https://doi.org/10.12989/amr.2017.6.4.317>
- Chergui, S., Daouadji, T.H., Hamrat, M., Boulekbache, B., Bougara, A., Abbes, B. and Amziane, S. (2019), "Interfacial stresses in damaged RC beams strengthened by externally bonded prestressed GFRP laminate plate: Analytical and numerical study", *Adv. Mater. Res., Int. J.*, **8**(3), 197-217. <https://doi.org/10.12989/amr.2019.8.3.197>
- Chikr, S.C., Kaci, A., Yeghnem, R. and Tounsi, A. (2019), "A new higher-order shear and normal deformation theory for the buckling analysis of new type of FGM sandwich plates", *Struct. Eng. Mech., Int. J.*, **72**(5), 653-673. <https://doi.org/10.12989/sem.2019.72.5.653>
- Daouadji, T.H. (2013), "Analytical analysis of the interfacial stress in damaged reinforced concrete beams strengthened by bonded composite plates", *Strength Mater.*, **45**(5), 587-597. <https://doi.org/10.1007/s11223-013-9496-4>
- Daouadji, H.T. (2017), "Analytical and numerical modeling of interfacial stresses in beams bonded with a thin plate", *Adv. Computat. Des., Int. J.*, **2**(1), 57-69. <https://doi.org/10.12989/acd.2017.2.1.057>
- Daouadji, H.T., Benyoucef, S., Tounsi, A., Benrahou, K.H. and Bedia, A.E. (2008), "Interfacial stress concentrations in FRP-damaged RC hybrid beams", *Compos. Interf.*, **15**(4), 425-440. <https://doi.org/10.1163/156855408784514702>
- Daouadji, T.H., Rabahi, A., Abbes, B. and Adim, B. (2016a), "Theoretical and finite element studies of interfacial stresses in reinforced concrete beams strengthened by externally FRP laminates plate", *J. Adhes. Sci. Technol.*, **30**(12), 1253-1280. <https://doi.org/10.1080/01694243.2016.1140703>
- Daouadji, T.H., Chedad, A. and Adim, B. (2016b), "Interfacial stresses in RC beam bonded with a functionally graded material plate", *Struct. Eng. Mech., Int. J.*, **60**(4), 693-705. <http://dx.doi.org/10.12989/sem.2016.60.4.693>
- Ghorbanpour Arani, A., Rousta Navi, B. and Mohammadimehr, M. (2016), "Surface stress and agglomeration effects on nonlocal biaxial buckling polymeric nanocomposite plate reinforced by CNT using various approaches", *Adv. Compos. Mater., Int. J.*, **25**(5), 423-441. <https://doi.org/10.1080/09243046.2015.1052189>
- Guenaneche, B. and Tounsi, A. (2014), "Effect of shear deformation on interfacial stress analysis in plated beams under arbitrary loading", *Adhes. Adhes.*, **48**, 1-13. <https://doi.org/10.1016/j.ijadhadh.2013.09.016>
- Hadj, B., Rabia, B. and Daouadji, T.H. (2019), "Influence of the distribution shape of porosity on the bending FGM new plate model resting on elastic foundations", *Struct. Eng. Mech., Int. J.*, **72**(1), 823-832. <https://doi.org/10.12989/sem.2019.72.1.061>
- Hadj, B., Rabia, B. and Daouadji, T.H. (2021), "Vibration analysis of porous FGM plate resting on elastic foundations: Effect of the distribution shape of porosity", *Coupl. Syst. Mech., Int. J.*, **10**(1), 61-77. <http://dx.doi.org/10.12989/csm.2021.10.1.061>
- Hamrat, M., Bouziadi, F., Boulekbache, B., Daouadji, T.H., Chergui, S., Labeled, A. and Amziane, S. (2020),

- “Experimental and numerical investigation on the deflection behavior of pre-cracked and repaired reinforced concrete beams with fiber-reinforced polymer”, *Constr. Build. Mater.*, **249**, 118745. <https://doi.org/10.1016/j.conbuildmat.2020.118745>
- He, X.J., Zhou, C.Y. and Wang, Y. (2019), “Interfacial stresses in reinforced concrete cantilever members strengthened with fibre-reinforced polymer laminates”, *Adv. Struct. Eng.*, **23**(2), 277-288. <https://doi.org/10.1177/1369433219868933>
- Hussain, M., Naeem, M.N., Taj, M. and Tounsi, A. (2020), “Simulating vibrations of vibration of single-walled carbon nanotube using Rayleigh-Ritz’s method”, *Adv. Nano Res., Int. J.*, **8**(3), 215-228. <https://doi.org/10.12989/anr.2020.8.3.215>
- Krou, B., Bernard, F. and Tounsi, A. (2014), “Fibers orientation optimization for concrete beam strengthened with a CFRP bonded plate: A coupled analytical-numerical investigation”, *Eng. Struct.*, **56**, 218-227. <https://doi.org/10.1016/j.engstruct.2013.05.008>
- Mahi, B.E., Benrahou, K.H., Belakhdar, K., Tounsi, A. and Bedia, E.A. (2014), “Effect of the tapered end of a FRP plate on the interfacial stresses in a strengthened beam used in civil engineering applications”, *Mech. Compos. Mater.*, **50**(4), 465-474. <https://doi.org/10.1007/s11029-014-9433-z>
- Mazars, J. and Pijaudier-Cabot, G. (1996), “From damage to fracture mechanics and conversely: A combined approach”, *Int. J. Solids Struct.*, **33**(20), 3327-3342. [https://doi.org/10.1016/0020-7683\(96\)00015-7](https://doi.org/10.1016/0020-7683(96)00015-7)
- Mohammadimehr, M. and Alimirzaei, S. (2016), “Nonlinear static and vibration analysis of Euler-Bernoulli composite beam model reinforced by FG-SWCNT with initial geometrical imperfection using FEM”, *Struct. Eng. Mech., Int. J.*, **59**(3), 431-454. <https://doi.org/10.12989/sem.2016.59.3.431>
- Mohammadimehr, M. and Mehrabi, M. (2018), “Electro-thermo-mechanical vibration and stability analyses of double-bonded micro composite sandwich piezoelectric tubes conveying fluid flow”, *Appl. Mathe. Modell.*, **60**, 255-272. <https://doi.org/10.1016/j.apm.2018.03.008>
- Mohammadimehr, M. and Meskini, M. (2020), “Analysis of porous micro sandwich plate: Free and forced vibration under magneto-electro-elastic loadings”, *Adv. Nano Res., Int. J.*, **8**(1), 69-82. <https://doi.org/10.12989/anr.2020.8.1.069>
- Mohammadimehr, M. and Shahedi, S. (2016), “Nonlinear magneto-electro-mechanical vibration analysis of double-bonded sandwich Timoshenko microbeams based on MSGT using GDQM”, *Steel Compos. Struct., Int. J.*, **21**(1), 1-36. <https://doi.org/10.12989/scs.2016.21.1.001>
- Mohammadimehr, M., Mohammadimehr, M.A. and Dashti, P. (2016a), “Size-dependent effect on biaxial and shear nonlinear buckling analysis of nonlocal isotropic and orthotropic micro-plate based on surface stress and modified couple stress theories using differential quadrature method”, *Appl. Mathe. Mech.*, **37**(4), 529-554. <https://doi.org/10.1007/s10483-016-2045-9>
- Mohammadimehr, M., Farahi, M.J. and Alimirzaei, S. (2016b), “Vibration and wave propagation analysis of twisted micro-beam using strain gradient theory”, *Appl. Mathe. Mech.*, **37**(10), 1375-1392. <https://doi.org/10.1007/s10483-016-2138-9>
- Mohammadimehr, M., Shahedi, S. and Rousta Navi, B. (2017a), “Nonlinear vibration analysis of FG-CNTRC sandwich Timoshenko beam based on modified couple stress theory subjected to longitudinal magnetic field using generalized differential quadrature method”, *Proceedings of the Institution of Mechanical Engineers, Part C: J. Mech. Eng. Sci.*, **231**(20), 3866-3885. <https://doi.org/10.1177/0954406216653622>
- Mohammadimehr, M., Navi, B.R. and Arani, A.G. (2017b), “Dynamic stability of modified strain gradient theory sinusoidal viscoelastic piezoelectric polymeric functionally graded single-walled carbon nanotubes reinforced nanocomposite plate considering surface stress and agglomeration effects under hydro-thermo-electro-magneto-mechanical loadings”, *Mech. Adv. Mater. Struct.*, **24**(16), 1325-1342. <https://doi.org/10.1080/15376494.2016.1227507>
- Mohammadimehr, M., Mohammadi-Dehabadi, A.A. and Maraghi, Z.K. (2017c), “The effect of non-local higher order stress to predict the nonlinear vibration behavior of carbon nanotube conveying viscous nanoflow”, *Physica B: Condens. Matt.*, **510**, 48-59. <https://doi.org/10.1016/j.physb.2017.01.0140>
- Mohammadimehr, M., Mohammadi-Dehabadi, A.A., Akhavan Alavi, S.M., Alambeigi, K., Bamdad, M., Yazdani, R. and Hanifehlou, S. (2018a), “Bending, buckling, and free vibration analyses of carbon nanotube

- reinforced composite beams and experimental tensile test to obtain the mechanical properties of nanocomposite”, *Steel Compos. Struct., Int. J.*, **29**(3), 405-422. <https://doi.org/10.12989/scs.2018.29.3.405>
- Mohammadimehr, M., Nejad, E.S. and Mehrabi, M. (2018b), “Buckling and vibration analyses of MGSGT double-bonded micro composite sandwich SSDT plates reinforced by CNTs and BNNTs with isotropic foam & flexible transversely orthotropic cores”, *Struct. Eng. Mech., Int. J.*, **65**(4), 491-504. <https://doi.org/10.12989/sem.2018.65.4.491>
- Mohammadimehr, M., Mehrabi, M., Hadizadeh, H. and Hadizadeh, H. (2018c), “Surface and size dependent effects on static, buckling, and vibration of micro composite beam under thermo-magnetic fields based on strain gradient theory”, *Steel Compos. Struct., Int. J.*, **26**(4), 513-531. <https://doi.org/10.12989/scs.2018.26.4.513>
- Mohammadimehr, M., Emdadi, M. and Roustavi, B. (2020), “Dynamic stability analysis of microcomposite annular sandwich plate with carbon nanotube reinforced composite facesheets based on modified strain gradient theory”, *J. Sandw. Struct. Mater.*, **22**(4), 1199-1234. <https://doi.org/10.1177/1099636218782770>
- Nejadi, M.M. and Mohammadimehr, M. (2020), “Buckling analysis of nano composite sandwich Euler-Bernoulli beam considering porosity distribution on elastic foundation using DQM”, *Adv. Nano Res., Int. J.*, **8**(1), 59-68. <https://doi.org/10.12989/anr.2020.8.1.059>
- Panjehpour, M., Ali, A.A.A., Voo, Y.L. and Aznieta, F.N. (2014), “Effective compressive strength of strut in CFRP-strengthened reinforced concrete deep beams following ACI 318-11”, *Comput. Concrete, Int. J.*, **13**(1), 135-165. <https://doi.org/10.12989/cac.2014.13.1.135>
- Panjehpour, M., Farzadnia, N., Demirboga, R. and Ali, A.A.A. (2016), “Behavior of high-strength concrete cylinders repaired with CFRP sheets”, *J. Civil Eng. Manage.*, **22**(1), 56-64. <https://doi.org/10.3846/13923730.2014.897965>
- Rabahi, A., Daouadji, T.H., Abbes, B. and Adim, B. (2016), “Analytical and numerical solution of the interfacial stress in reinforced-concrete beams reinforced with bonded prestressed composite plate”, *J. Reinf. Plast. Compos.*, **35**(3), 258-272. <https://doi.org/10.1177/0731684415613633>
- Rabia, B., Abderezak, R., Daouadji, T.H., Abbes, B., Belkacem, A. and Abbes, F. (2018), “Analytical analysis of the interfacial shear stress in RC beams strengthened with prestressed exponentially-varying properties plate”, *Adv. Mater. Res., Int. J.*, **7**(1), 29-44. <https://doi.org/10.12989/amr.2018.7.1.029>
- Rabia, B., Daouadji, T.H. and Abderezak, R. (2019), “Effect of distribution shape of the porosity on the interfacial stresses of the FGM beam strengthened with FRP plate”, *Earthq. Struct., Int. J.*, **16**(5), 601-609. <https://doi.org/10.12989/eas.2019.16.5.601>
- Rabia, B., Daouadji, T.H. and Abderezak, R. (2021), “Effect of air bubbles in concrete on the mechanical behavior of RC beams strengthened in flexion by externally bonded FRP plates under uniformly distributed loading”, *Compos. Mater. Eng.*, **3**(1), 41-55. <http://dx.doi.org/10.12989/cme.2021.3.1.041>
- Rabahi, A., Adim, B., Chargui, S. and Daouadji, T.H. (2014), “Interfacial stresses in FRP-plated RC beams: effect of adherend shear deformations”, *Proceedings of Conference on Multiphysics Modelling and Simulation for Systems Design*, Volume 2, pp. 317-326. https://doi.org/10.1007/978-3-319-14532-7_33
- Rajabi, J. and Mohammadimehr, M. (2019), “Bending analysis of a micro sandwich skew plate using extended Kantorovich method based on Eshelby-Mori-Tanaka approach”, *Comput. Concrete, Int. J.*, **23**(5), 361-376. <https://doi.org/10.12989/cac.2019.23.5.361>
- Rostami, R. and Mohammadimehr, M. (2020), “Vibration control of rotating sandwich cylindrical shell-reinforced nanocomposite face sheet and porous core integrated with functionally graded magneto-electro-elastic layers”, *Eng. Comput.*, 1-14. <https://doi.org/10.1007/s00366-020-01052-5>
- Shahedi, S. and Mohammadimehr, M. (2020), “Nonlinear high-order dynamic stability of AL-foam flexible cored sandwich beam with variable mechanical properties and carbon nanotubes-reinforced composite face sheets in thermal environment”, *J. Sandw. Struct. Mater.*, **22**(2), 248-302. <https://doi.org/10.1177/1099636217738908>
- Sharif, A.M., Assi, N.A. and Al-Osta, M.A. (2020), “Use of UHPC slab for continuous composite steel-concrete girders”, *Steel Compos. Struct., Int. J.*, **34**(3), 321-332. <https://doi.org/10.12989/scs.2020.34.3.321>

- Smith, S.T. and Teng, J.G. (2002), "Interfacial stresses in plated beams", *Eng. Struct.*, **23**(7), 857-871. [http://dx.doi.org/10.1016/S0141-0296\(00\)00090-0](http://dx.doi.org/10.1016/S0141-0296(00)00090-0)
- Tahar, H.D., Boussad, A., Abderezak, R., Rabia, B., Fazilay, A. and Belkacem, A. (2019), "Flexural behaviour of steel beams reinforced by carbon fibre reinforced polymer: Experimental and numerical study", *Struct. Eng. Mech., Int. J.*, **72**(4), 409-419. <https://doi.org/10.12989/sem.2019.72.4.409>
- Tahar, H.D., Abderezak, R. and Rabia, B. (2020), "Flexural performance of wooden beams strengthened by composite plate", *Struct. Monitor. Maint., Int. J.*, **7**(3), 233-259. <http://dx.doi.org/10.12989/smm.2020.7.3.233>
- Tayeb, B. and Daouadji, T.H. (2020), "Improved analytical solution for slip and interfacial stress in composite steel-concrete beam bonded with an adhesive", *Adv. Mater. Res., Int. J.*, **9**(2), 133-153. <https://doi.org/10.12989/amr.2020.9.2.133>
- Tayeb, T.S., Zidour, M., Bensattalah, T., Heireche, H., Benahmed, A. and Bedia, E.A. (2020), "Mechanical buckling of FG-CNTs reinforced composite plate with parabolic distribution using Hamilton's energy principle", *Adv. Nano Res., Int. J.*, **8**(2), 135-148. <https://doi.org/10.12989/anr.2020.8.2.135>
- Tlidji, Y., Benferhat, R. and Tahar, H.D. (2021), "Study and analysis of the free vibration for FGM microbeam containing various distribution shape of porosity", *Struct. Eng. Mech., Int. J.*, **77**(2), 217-229. <http://dx.doi.org/10.12989/sem.2021.77.2.217>
- Tounsi, A. (2006), "Improved theoretical solution for interfacial stresses in concrete beams strengthened with FRP plate", *Int. J. Solids Struct.*, **43**(14-15), 4154-4174. <https://doi.org/10.1016/j.ijsolstr.2005.03.074>
- Tounsi, A., Daouadji, T.H. and Benyoucef, S. (2008), "Interfacial stresses in FRP-plated RC beams: Effect of adherend shear deformations", *Int. J. Adhes. Adhes.*, **29**, 313-351. <https://doi.org/10.1016/j.ijadhadh.2008.06.008>
- Tounsi, A., Al-Dulaijan, S.U., Al-Osta, M.A., Chikh, A., Al-Zahrani, M.M., Sharif, A. and Tounsi, A. (2020), "A four variable trigonometric integral plate theory for hygro-thermo-mechanical bending analysis of AFG ceramic-metal plates resting on a two-parameter elastic foundation", *Steel Compos. Struct., Int. J.*, **34**(4), 511-524. <https://doi.org/10.12989/scs.2020.34.4.511>
- Yang, J. and Wu, Y.F. (2007), "Interfacial stresses of FRP strengthened concrete beams: Effect of shear deformation", *Compos. Struct.*, **80**, 343-351. <https://doi.org/10.1016/j.compstruct.2006.05.016>
- Zohra, A., Benferhat, R., Tahar, H.D. and Tounsi, A. (2021), "Analysis on the buckling of imperfect functionally graded sandwich plates using new modified power-law formulations", *Struct. Eng. Mech., Int. J.*, **77**(6), 797-807. <http://dx.doi.org/10.12989/sem.2021.77.6.797>